Electromagnetic Transient Modeling of Form-Wound Stator Coils with Stress Grading System under PWM excitation

Mohammed Khalil Hussain, Pablo Gomez, Fermin P. Espino-Cortes

Abstract-- **The insulation system of a machine coil includes several layers made of materials with different characteristics. The effective insulation design of machine coils, especially in the machine end winding, depends upon an accurate model of the stress grading system. This paper proposes a modeling approach to predict the transient overvoltage, electric field, and heat generation in machine coils with a stress grading system, considering the variation of physical properties in the insulation layers. A non-uniform line model is used to divide the coil in different segments based on material properties and lengths: overhang, stress grading and slot. The cascaded connection of chain matrices is used to connect segments for the representation of the complete machine coil. The resulting model is able to simulate the transient overvoltages due to the application of fast rise time pulses such as those observed with pulse width modulation from adjustable speed drives, considering coils with different insulation topologies and under pulses with different rise times. The parameters in each coil region are calculated using the finite element method (FEM). Additionally, the resistive heat and electric field distribution in the machine coil are calculated for excitations with different rise times by means of 3-dimensional FEM simulations.**

Keywords: **Rotating machine, form-wound stator coil, stress grading system, non-uniform transmission line model.**

I. INTRODUCTION

AC rotating machines are subjected to fast front pulses when fed from frequency converters. Even though this type of excitation is used to improve the efficiency of the machine, it produces dielectric stress in the machine winding that can result in premature deterioration or even failure [1]-[3]. The reliability of high voltage rotating machines depends mainly on the strength of the insulation system [4], [5]. Insulation breakdown of machine winding is a critical condition that often results in significant costs due to repairs, replacements, or outages. One of the main reasons for breakdown in high voltage rotating machine is the failure of the stator insulation [1], [4], [5].

Form-wound stator coils utilize two types of stress control layers in the insulation system: semi-conductive armor tape (CAT) in the slot region, and stress grading tape (SGT) in the stator end windings [6]. CAT is used to prevent electrical discharges occurring along the coil surface and air gaps between the coil surface and laminated core [7]. SGT is used to control the electric field (E) at the end of the CAT insulation to prevent damage in the ground wall insulation [1]. As a part of standard acceptance testing in machine winding, it is required that the high voltage winding passes high blackout testing at a level ranging from 100% to 150% of the nominal line-to-ground voltage without visual partial discharge [5]. Also, it is required to pass 200% line-to-ground blackout testing without any visual corona discharge and no repairs on the stress grading system [1], [5].

The insulation system design of machine coils must take into account the physical characteristics of insulation layers such as grading layers, material properties, and geometrical arrangement [8]. The use of increasingly faster front pulses from PWM-based adjustable speed drives have compelled manufactures to increase the insulation level, particularly in the stress grading system, to reduce the possibility of insulation failure [1], [8]. Detailed models of machine coils can be either based on constant-lumped-parameter or distributed-parameter representations. Previous distributed parameter models have not included the effect of the stress grading system in the transient performance of machine windings [9]-[11]. On the other hand, constant-lumped parameter models proposed so far have not considered the complex physical properties of the coil's insulation system [4], [5], [12], [13]. A lumped-parameter model based on series impedance and shunt admittance elements connected in cascade is used in [5] to describe the stress-grading and the slot regions of the coil, respectively. Also, a lumped-parameter model that includes nonlinear resistances and shunt capacitors in series connection is presented in [4] to represent the end-turn zone of a high voltage coil. Similarly, in [12] shunt capacitors and field-dependent series resistances are used to represent the stress-grading system model. An RC ladder circuit model is also used as an equivalent circuit of the SG system in [13].

This paper proposes a modeling approach to predict the transient voltage distribution, electric field, and heat generation along a machine winding with a stress grading system, fed by a fast front excitation from a PWM source. A nonuniform transmission line model is used to simulate the variation of pulse propagation in the insulation layers of the machine coil: slot, stress grading, and overhang regions. The parameters of the coil based on a nonuniform transmission line representation are calculated from the application of finite element analysis considering the different physical characteristics of the insulation layers.

M. K. Hussain is with Department of Energy Engineering, University of Baghdad, Baghdad, Iraq (e-mail: mohammedkhalil@uobaghdad.edu.iq).

P. Gómez is with the Department of Electrical and Computer Engineering, Western Michigan University, Kalamazoo, MI 49008 USA (e-mail: pablo.gomez@wmich.edu).

F. P. Espino-Cortés is with the Graduate Program in Electrical Engineering, SEPI-ESIME Zacatenco, Instituto Politécnico Nacional, Mexico City, 07738 Mexico (e-mail: fespinoc@ipn.mx).

## II. Insulation System in Form-Wound Stator Coil

The form-wound coils of a rotating machine are distributed around the stator. A coil can be divided into four main regions based on different insulation layers and different lengths: overhang (OH), slot (SL), stress grading (SG), and double overhang (DOH), as shown in Fig. 1.
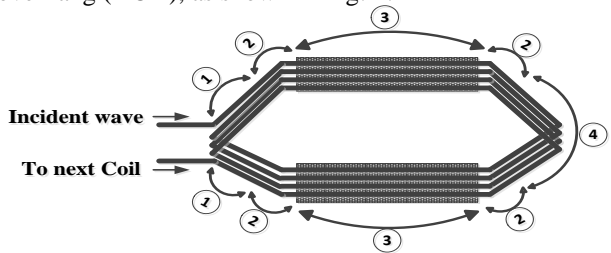
1- Overhang Region 2- Stress Grading Region
3- Slot Region 4- Double Overhang Region

Fig. 1.   Machine coil regions (3 turns considered for illustration)

The form-wound stator coil consists of copper conductors of rectangular cross-section covered by different insulation layers. As shown in Fig. 2, the insulation system of the machine coil has five different layers: inter-turn insulation, main insulation, ground wall insulation, corona armor tape (CAT), and stress grading tape (SGT). Each layer has different geometrical and material properties [14].
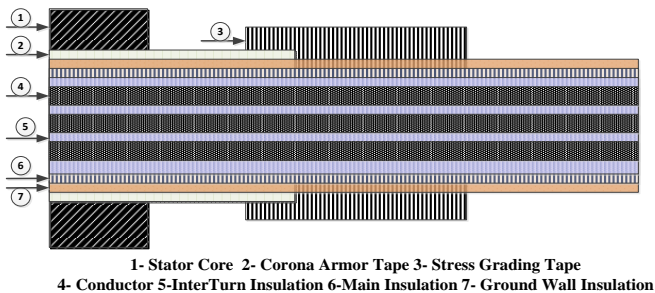
1- Stator Core 2- Corona Armor Tape 3- Stress Grading Tape
4- Conductor 5-InterTurn Insulation 6-Main Insulation 7- Ground Wall Insulation

Fig. 2. Cross-sectional view of coil (3 turns considered for illustration).

III. Modeling Approach

The stress grading tape of the machine coil is used to prevent partial discharges in the ground wall insulation [1]. The permittivity of the insulation layers is higher than the permittivity of air. The variation between these permittivities can produce a high electric field and partial discharges in the overhang region. To control the stress at the end of the CAT, SGT is used to modify the surface impedance of the ground wall insulation [1]. Usually, the modeling of CAT and SGT in the machine coil is done separately. To analyze the effect of different rise times of the PWM excitation in the transient overvoltage, electric field, and resistive heat generation on the machine coil, it is important to model the SG and CAT regions together in the machine winding model [1]. For this reason, a frequency-domain, non-uniform transmission line model is applied to simulate the transient response of the machine coil with a stress grading system under fast front excitation. This model allows considering the frequency dependence of the coil's electrical parameters due to the presence of eddy currents, as well as their space dependence due to the use of different insulation materials in the regions depicted in Fig. 1 [10], [15].

A. Machine Coil Model Based on Non-Uniform Transmission Line

This model divides the machine coil, based on different insulation layers and different lengths, in four main regions: overhang (OH), stress grading (SG), slot (SL), and double overhang (DOH). The voltage and current propagation along the nonuniform transmission line model in the frequency domain is defined as follows [16]:

$$\frac{d}{dx}\begin{bmatrix} \mathbf{V}(x,s) \\ \mathbf{I}(x,s) \end{bmatrix} = \begin{bmatrix} 0 & -\mathbf{Z}(x,s) \\ -\mathbf{Y}(x,s) & 0 \end{bmatrix}\begin{bmatrix} \mathbf{V}(x,s) \\ \mathbf{I}(x,s) \end{bmatrix} \quad (1)$$

$$\mathbf{Z}(x,s) = \mathbf{R}(x,s) + s\mathbf{L}(x,s) \quad (2)$$

$$\mathbf{Y}(x,s) = \mathbf{G}(x,s) + s\mathbf{C}(x,s) \quad (3)$$

where $\mathbf{V}(x,s)$ and $\mathbf{I}(x,s)$ are the voltage and current vectors in the Laplace domain (s) at any point x, $\mathbf{Z}(x,s)$ and $\mathbf{Y}(x,s)$ are the longitudinal impedance and transversal admittance matrices per-unit length. $\mathbf{R}(x,s)$, $\mathbf{L}(x,s)$, $\mathbf{C}(x,s)$ and $\mathbf{G}(x,s)$ are the resistance, inductance, capacitance, and conductance matrices per unit length, respectively.

The parameters $\mathbf{Z}(x,s)$ and $\mathbf{Y}(x,s)$ of the machine coil are in general frequency and space-dependent according to (1)-(3). However, the electrical parameters are assumed constant with space for each insulation section of the machine.

Assuming a section of length Δx, the chain matrix model for this section is obtained by applying the boundary conditions at x and $x+\Delta x$ to (1), which yields the following two-port representation [11], [16]:

$$\begin{bmatrix} \mathbf{V}(x + \Delta x, s) \\ \mathbf{I}(x + \Delta x, s) \end{bmatrix} = \boldsymbol{\phi}(\Delta x, s)\begin{bmatrix} \mathbf{V}(x,s) \\ \mathbf{I}(x,s) \end{bmatrix} \quad (4)$$

where

$$\boldsymbol{\phi}(\Delta x, s) = \begin{bmatrix} \cosh(\boldsymbol{\psi}\Delta x) & -\mathbf{Y}_0^{-1}\sinh(\boldsymbol{\psi}\Delta x) \\ -\mathbf{Y}_0\sinh(\boldsymbol{\psi}\,\Delta x) & \mathbf{Y}_0\cosh(\boldsymbol{\psi}\Delta x)\mathbf{Y}_0^{-1} \end{bmatrix} \quad (5)$$

$$\boldsymbol{\psi} = \mathbf{M}\sqrt{\boldsymbol{\lambda}}\,\mathbf{M}^{-1} \quad (6)$$

$$\mathbf{Y}_0 = \mathbf{Z}(x,s)^{-1}\boldsymbol{\psi} \quad (7)$$

where $\mathbf{M}$ and $\boldsymbol{\lambda}$ are the eigenvector and eigenvalue matrices of the matrix product $\mathbf{Z}(x,s)\mathbf{Y}(x,s)$.

B. Cascaded Connection of Chain Matrices

The machine coil model is divided into four regions based on the different geometrical and physical properties of insulation layers, as shown in Fig.3. In this figure, $\mathbf{V}_S$ and $\mathbf{I}_S$ represent the voltage at the sending node of the coil, while $\mathbf{V}_R$ and $\mathbf{I}_R$ correspond to the voltage and current and the receiving node. The stress grading region is divided into three segments: stress grading tape (SGT), overlap region (OL), and corona armor tape (CAT), as shown in Fig. 4.
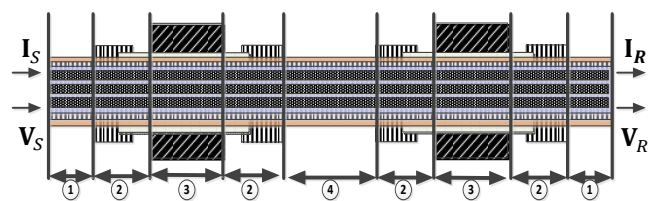
1- Overhang (OH) 2-Stress Grading (SG) 3- slot (SL) 4- Double Overhang (DOH)

Fig. 3. Representation of machine coil (3 turns considered for illustration).
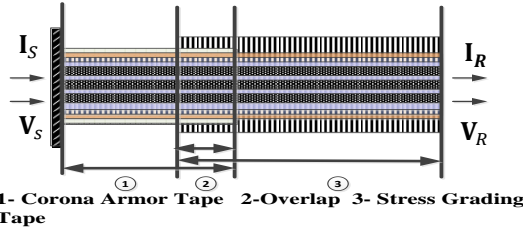
Fig. 4. Representation of SG system (3 turns considered for illustration).

Each part of the machine coil can be represented as a chain matrix according to (5). This equation is a function of the parameters $\mathbf{Z}$ and $\mathbf{Y}$, which are different in each region of the machine coil. The method of cascaded connection of chain matrices is applied to obtain the equivalent chain matrix that represents the complete coil, as illustrated in Fig. 5. The relationship between the sending and receiving nodes of the complete coil model is obtained as

$$\begin{bmatrix} \mathbf{V}_R \\ \mathbf{I}_R \end{bmatrix} = \boldsymbol{\phi}_{OH}\boldsymbol{\phi}_{SG1}\boldsymbol{\phi}_{SL}\boldsymbol{\phi}_{SG2}\boldsymbol{\phi}_{DOH}\boldsymbol{\phi}_{SG1}\boldsymbol{\phi}_{SL}\boldsymbol{\phi}_{SG2}\boldsymbol{\phi}_{OH}\begin{bmatrix} \mathbf{V}_S \\ \mathbf{I}_S \end{bmatrix}$$
$$= \begin{bmatrix} \boldsymbol{\Phi}_{11} & \boldsymbol{\Phi}_{12} \\ \boldsymbol{\Phi}_{21} & \boldsymbol{\Phi}_{22} \end{bmatrix}\begin{bmatrix} \mathbf{V}_S \\ \mathbf{I}_S \end{bmatrix}$$

(8)
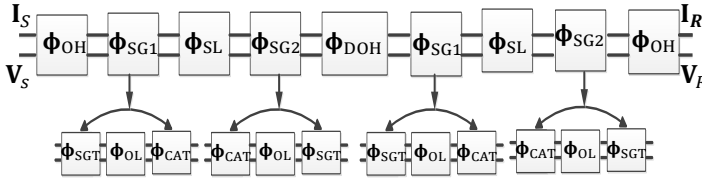
Fig. 5. Cascaded connection of chain matrices to model all regions of machine coil

where $\boldsymbol{\phi}_{SG1} = \boldsymbol{\phi}_{SGT}\boldsymbol{\phi}_{OL}\boldsymbol{\phi}_{CAT}$, $\boldsymbol{\phi}_{SG2} = \boldsymbol{\phi}_{CAT}\boldsymbol{\phi}_{OL}\boldsymbol{\phi}_{SGT}$, and $\boldsymbol{\Phi}_{11}$, $\boldsymbol{\Phi}_{12}$, $\boldsymbol{\Phi}_{21}$ and $\boldsymbol{\Phi}_{22}$ are the elements (submatrices) of the chain matrix of the complete coil. This matrix is transformed into an equivalent nodal (admittance) form. Then, a zig-zag connection is applied between turns to preserve continuity as the incident wave propagates along the coil turns [11]. This yields

$$\begin{bmatrix} \mathbf{V}_S \\ \mathbf{V}_R \end{bmatrix} = \begin{bmatrix} \mathbf{Y}_{SS} + \mathbf{Y}_{con11} & -(\mathbf{Y}_{SR} + \mathbf{Y}_{con12}) \\ -(\mathbf{Y}_{SR} + \mathbf{Y}_{con21}) & \mathbf{Y}_{RR} + \mathbf{Y}_{con22} \end{bmatrix}^{-1}\begin{bmatrix} \mathbf{I}_S \\ \mathbf{I}_R \end{bmatrix}$$

(9)

where

$$\mathbf{Y}_{SS} = -\boldsymbol{\Phi}_{12}^{-1}\boldsymbol{\Phi}_{11} \tag{10}$$
$$\mathbf{Y}_{SR} = -\boldsymbol{\Phi}_{12}^{-1} = -\boldsymbol{\Phi}_{22}\boldsymbol{\Phi}_{12}^{-1}\boldsymbol{\Phi}_{11} + \boldsymbol{\Phi}_{21} \tag{11}$$
$$\mathbf{Y}_{RR} = -\boldsymbol{\Phi}_{22}\boldsymbol{\Phi}_{12}^{-1} \tag{12}$$

The definition of the connection matrices required to perform the of zig-zag connection ($\mathbf{Y}_{con11}$, $\mathbf{Y}_{con12}$, $\mathbf{Y}_{con21}$, and $\mathbf{Y}_{con22}$) can be found in [18]. The frequency domain voltages in (9) are transformed into the time domain by means of the inverse numerical Laplace transform (INLT) [17]. This tool has been widely used for electromagnetic transient analysis of power components and systems when frequency domain modeling methods are applied. The INLT can be regarded as a modified version of the inverse fast Fourier transform to avoid aliasing errors and Gibbs oscillations due to the discretization and truncation of the frequency spectrum.

C. Parameter Computation Using FEM

The elements of the capacitance, inductance, and dielectric losses matrices in each different region of the machine coil are calculated using the FEM-based simulation program COMSOL Multiphysics [18]. The capacitance matrix in the machine coil is calculated using the forced voltage method. The inductance matrix is calculated using the magnetic energy method. The concept of complex penetration depth is used to calculate the series losses in the machine coil ($\mathbf{R}$). The dielectric losses matrix ($\mathbf{G}$) is computed using the "electric currents" module in COMSOL. The permittivity and conductivity of each insulation layer of the machine coil are required in losses calculations. The nonlinear conductivity of SGT is defined as a function of the electric field, E [1]:

$$\sigma(E) = \sigma_0\, e^{\alpha E} \tag{13}$$

where σ_0 and α are positive constants obtained from experimental data [1].

IV. CASE STUDY

A. Geometrical Configuration

The winding under analysis corresponds to a form-wound stator coil. It consists of seven conductors with five insulation layers: inter-turn insulation, main insulation, ground wall insulation, corona armor tape (CAT), and stress grading tape (SGT) [9], [11]. Fig. 6. shows the cross-section of the coil considered in this study. The main parameters of the stator coil are summarized in Table I. Table II shows the electric field characteristics of the stress grading system.

B. Computation of Electrical Parameters

For the purpose of parameter computation, a single coil can be divided in three main regions based on insulation characteristics: overhang (OH), stress grading (SG), and slot (SL). The stress grading region is divided in three segments: stress grading tape (SGT), overlap (OL), and corona armor tape (CAT). The capacitance, inductance, and losses matrices in these regions are calculated using the FEM-based software COMSOL Multiphysics, as explained in Section III.C.
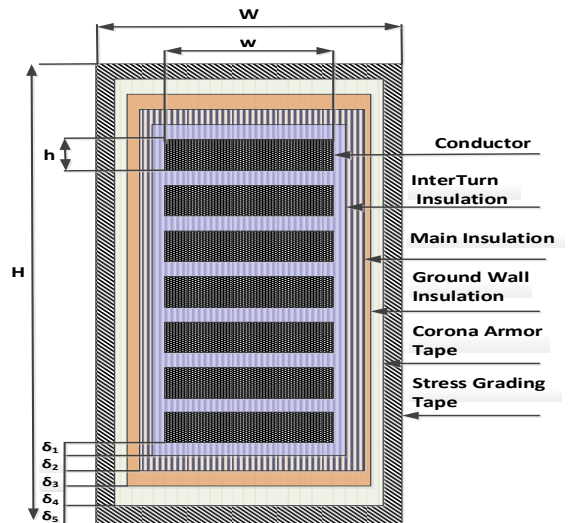

Fig. 6. Cross-sectional view of the machine coil with insulation layers.

TABLE I
MAIN COIL PARAMETERS.

Parameter	Value
Turns per stator coil	7
Slot length	0.5 m
Length of total overhang region	0.22m
Length of CAT after slot	0.08 m
Length of (SGT)	0.09m
Length of (OL)	0.02m
Conductor width (w)	5.35 mm
Conductor height (h)	2.85 mm
Resistivity of the stator bar conductor	1.7×10^{-8} Ω-m
Thickness of inter-turn insulation (δ_1)	0.2 mm
Thickness of the main insulation (δ_2)	1.41 mm
Thickness of ground wall insulation (δ_3)	0.36 mm
Thickness of CAT insulation (δ_4)	0.488 mm
Thickness of SGT insulation (δ_5)	0.848 mm
Relative permittivity of the inter-turn Ins.	2.5
Relative permittivity of the main Ins.	2
Relative permittivity of ground wall Ins.	2.8
Relative permittivity of stress grading tape	2.6
Relative permittivity of corona armor tape	100
Slot width (W)	10.07 mm
Slot height (H)	25.87 mm

TABLE II
PROPERTIES OF MATERIALS FOR MACHINE COIL.

Material	Electrical conductivity (S/m)
Insulation layers	2×10^{-15}
CAT	0.32
SGT	$3.38 \times 10^{-6} \exp (6.88 \times 10^{-6} \times E)$

Figs. 7 and 8 show the calculation of self-capacitance from forced voltage method and self-inductance from magnetic energy using COMSOL Multiphysics. Mutual elements are calculated in a similar manner, but exciting two turns at a time, as explained in [15]. Mutual capacitances and inductances between turns from different slots are neglected assuming that the stronger electromagnetic couplings appear between turns within each slot.

C. Computation of Transient Overvoltage

Fig. 9 shows the setup of the form-wound coil under test. This figure shows a waveform generator as a PWM source, and a 100 Ω load (R) connected at the end of the coil (representing the approximate impedance of the rest of the winding). The voltage applied is a step waveform characterized by a magnitude of 1750 V and a rise time varied from 25 and 100 ns. The peak-value of 1750 V is typical for square-wave-pulse testing of form-wound inverter-fed AC motors (see for instance [19]-[21]. The range of rise times under consideration are selected since they are expected in the next generation of power electronic converters [22].

The voltage source is injected directly to the beginning of the machine winding. The waveforms in Figs. 10 and 11 show the distribution of transient overvoltage along the machine coil for 25 ns and 100 ns rise time, respectively. These figures show that the transient overvoltages decrease as the rise time is increased.

The dielectric stress produced by the fast front excitation between turns is directly related to the potential difference between turns. Fig. 12 illustrates the maximum potential difference between adjacent turns for excitations with different

rise times. This is computed from the transient overvoltage for the 6 different rise times considered. It can be noticed in Fig. 12 that the largest potential differences occur with 25 ns of rising time, and these values are reduced as the rise time is increased.
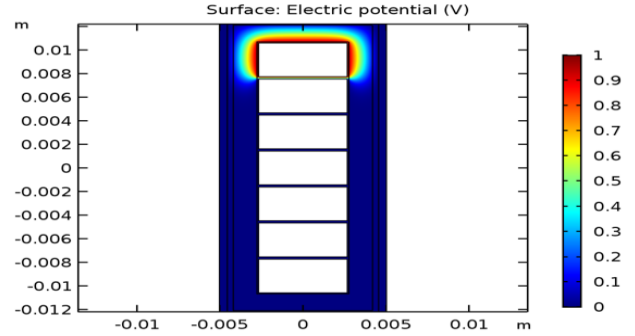

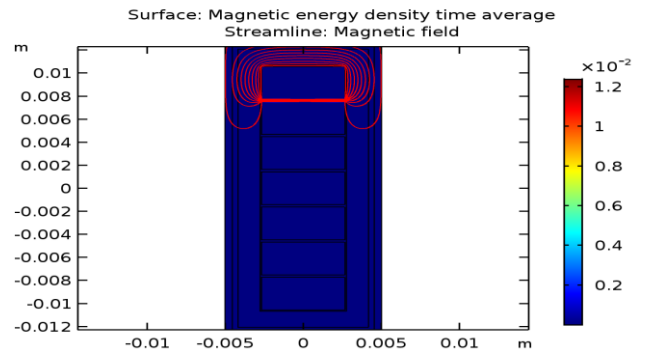Fig. 7. Capacitance calculation in FEM.
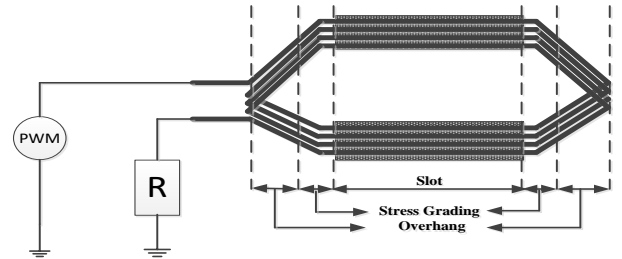

Fig. 8. Inductance calculation in FEM.

Fig. 9. Schematic model of a form-wound stator coil (3 turns considered for illustration purposes).
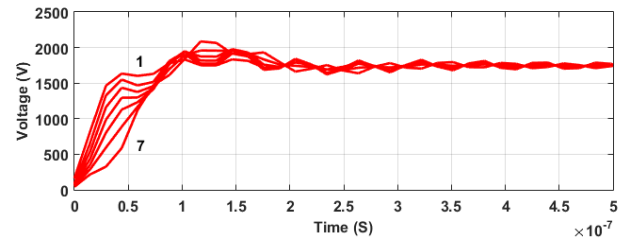

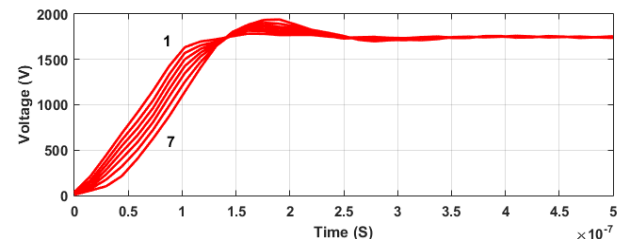Fig. 10. Transient overvoltage in 25 ns rise time excitation.

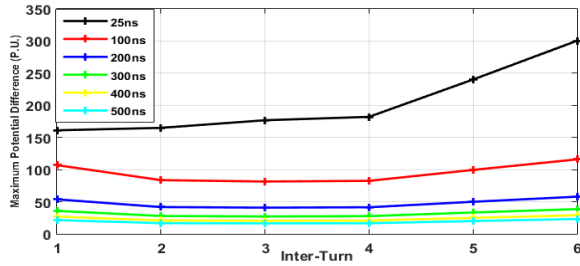Fig. 11. Transient overvoltage in 100 ns rise time excitation.

Fig. 12. The maximum potential difference in different rise times.

D. Computation of Electric Field and Resistive Heat Density

To calculate the maximum electric field in the machine coil, the potential in each turn is extracted from the transient overvoltage at the time of maximum potential difference between adjacent turns:

$$\mathbf{V}_{turns} = \max \left\{ \begin{bmatrix} V_1 - V_2 \\ V_2 - V_3 \\ \vdots \\ V_{n-1} - V_n \end{bmatrix} \right\} \quad (14)$$

where n is the number of turns in the machine coil. The potential of each turn shown in Fig. 13 is applied at each turn of the coil by using a 3D geometry in COMSOL Multiphysics, as illustrated in Fig. 14.
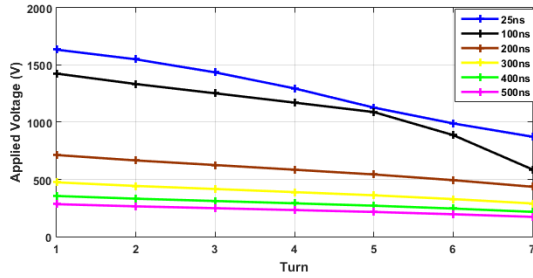
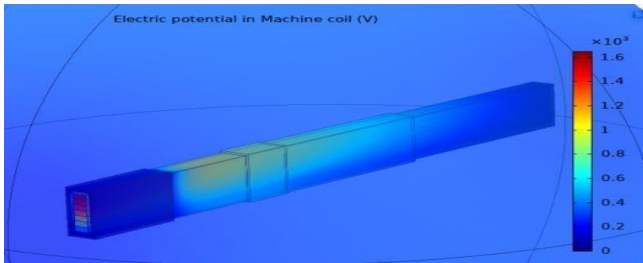Fig. 13. Turn-to-ground voltage applied at each turn of the machine coil

Fig. 14. 3D geometry in COMSOL for excitation with 25 ns rise time.

Fig. 15 shows the maximum electric field on the top surface of the machine coil at different rise times. This figure shows the electric field distribution in the machine coil, which decreases as rise time is increased. Fig. 16 shows the maximum resistive heat density on the top surface of the machine coil at different rise times. This figure shows that the maximum resistive heat density is decreased as rise time is increased.

Figs. 17 and 18 show the maximum electric field and the maximum resistive heat density on the bottom surface of the machine coil at different rise times. As shown in both of these figures, the maximum electric field and resistive heat density are increased with the voltage applied to the coil turns.
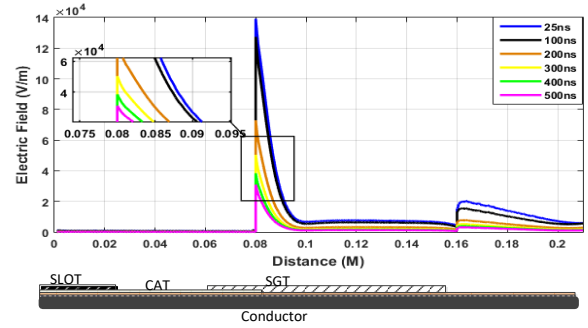

Fig. 15. Maximum Electric field distribution on the top surface of the coil.
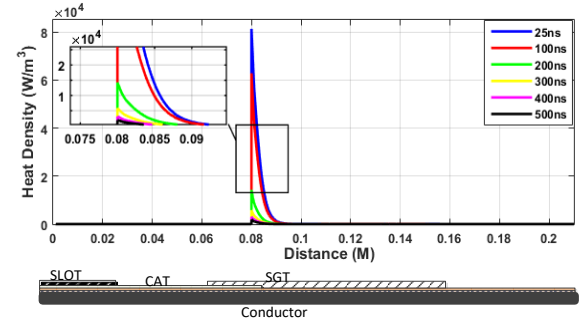

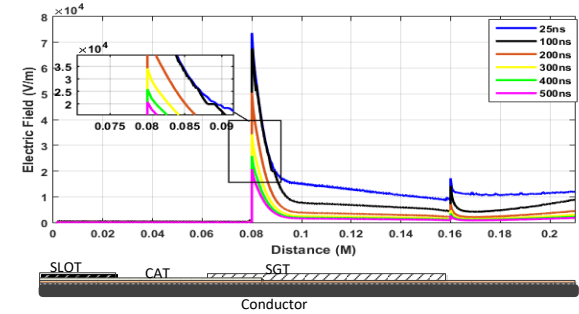Fig. 16. Maximum resistive heat density on the top surface of the coil.

Fig. 17. Maximum Electric field distribution on the bottom surface of the coil.
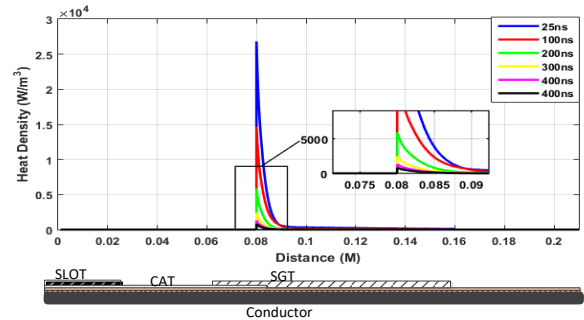

Fig. 18. Maximum resistive heat density on the bottom surface of the coil.

E. Changing the Physical Properties of Insulation Layers

This section shows the effect of changing the physical properties of the insulation layers in the electrical and thermal behavior of the machine coil. Figs. 19 and 20 show the electrical and thermal distribution along the machine coil when applying three different relative permittivities for the main insulation (2, 3, 4) and an excitation with 25 ns of rise time. These figures show that both electric and thermal fields are affected by the relative permittivity of the main insulation.
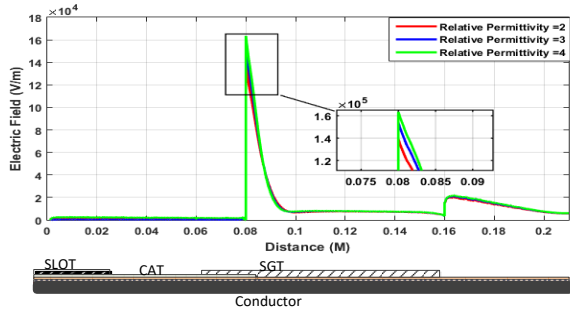
Fig. 19. Maximum electric field distribution on the surface of the coil with different relative permittivities.
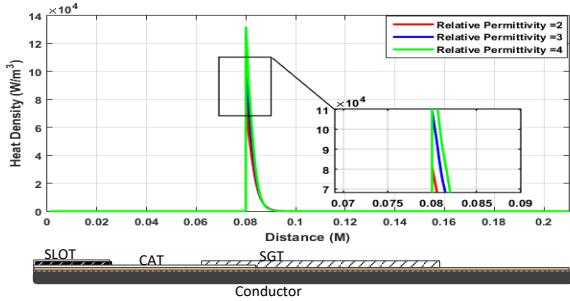

Fig. 20. Maximum resistive heat density in the surface of the coil with different relative permittivities.

The nonlinearity of the stress grading tape (SGT) is modified by considering three different values of $\propto$ ($\propto_1 = 1 \times 10^{-6}$, $\propto_2 = 3.38 \times 10^{-6}$, $\propto_3 = 9 \times 10^{-6}$) [13]. The conductivity (σ) in the stress grading system is defined as a function of the electric field (E) and $\propto$ [1]:

$$\sigma = 3.38 \times 10^{-6} \times e^{\alpha E} \qquad (15)$$

Figs. 21 and 22 show the distribution of electric and thermal stresses along the machine coil. As shown in these figures, the electric field decreases when the level of nonlinearity increases, while the heat generation in the SGT increases by increasing its level of the nonlinearity.
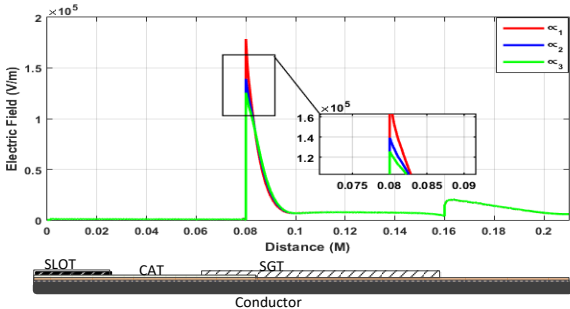

Fig. 21. Maximum electric field distribution on the top surface of the coil as a function of SG nonlinearity.
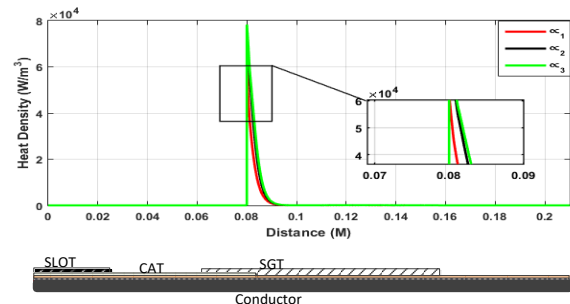

Fig. 22. Maximum resistive heat density in the top surface of the machine coil.

F. Experimental verification

The winding model including stress grading system has been previously validated experimentally in [9]. A PWM-type excitation with different rise times was connected to the first turn of a form-wound coil. The end of the last turn of the coil was connected to a resistor of $100 \; \Omega$ to represent the rest of the winding. The results obtained in [9] evidence the accuracy of the coil model when compared with laboratory measurements.

V. CONCLUSIONS

This paper presents a method to predict the transient overvoltages, electric field distribution, and heat generation of a machine winding with stress grading system. A nonuniform multiconductor transmission line model in the frequency domain was used to represent the complete machine coil considering the variation in geometrical and electrical properties among the layers of the insulation system. The parameters of the coil were calculated using COMSOL Multiphysics. The results when applying a PWM-type excitation to the coil show that the rise time of the source and the characteristics of insulation layers have an important effect on the transient overvoltage produced at different turns of the coil, the potential difference between adjacent turns, the electrical field in the surface of the coil, and the heat generation in the machine coil. The comparison between simulation and experimental results shows an adequate approximation for fast transient studies. The nonuniform transmission line representation in the frequency domain is an efficient approach for machine coil modeling to study the transient propagation response of the form-wound machine coil with stress grading system.

VI. REFERENCES

[1] F. P. Espino-Cortes, E. A. Cherney and S. Jayaram, "Effectiveness of stress grading coatings on form-wound stator coil groundwall insulation under fast rise time pulse voltages," IEEE Transactions on Energy Conversion, vol. 20, no. 4, pp. 844-851, Dec. 2005.

[2] T. Nakamura et al, "Optimal resistance of stress grading system in converter-fed rotating machines," 2016 IEEE Conference on Electrical Insulation and Dielectric Phenomena (CEIDP), Toronto, pp. 15-18.

[3] T. Nakamura et al, "Transient potential measurement on stress grading under multi-level PWM,"2015 IEEE Electrical Insulation Conference (EIC), pp. 161-165.

[4] F. P. Espino-Cortes, P. Gomez and J. D. Betanzos Ramirez, "Modeling of heat generated on stress grading coatings of motors fed by multilevel drives," IEEE Transactions on Dielectrics and Electrical Insulation, vol. 18, no. 4, pp. 1328-1333, August 2011.

[5] H. El-Kishky, M. Abdel-Salam, H. Wedaa and Y. Sayed, "Time-domain analysis of nonlinear stress-grading systems for high voltage rotating machines," 2003 IEEE Annual Report Conference on Electrical Insulation and Dielectric Phenomena, Albuquerque, pp. 482-485.

[6] R. Omranipour and S. U. Haq, "Evaluation of Grading System of Large Motors AC Stator Windings," 2008 IEEE International Symposium on Electrical Insulation, pp. 158-161.

[7] S. Ul Haq and R. Omranipour, "Comparative evaluation of various grading systems for electric machinery stator windings," 2010 IEEE International Symposium on Electrical Insulation, pp. 1-4.

[8] A. E. Baker, A. M. Gully and J. C. G. Wheeler, "Finite element modelling of nonlinear stress grading materials for machine end windings," 2002 International Conference on Power Electronics, Machines and Drives, pp. 265-268.

[9] M. K. Hussain and P. Gomez, "Modeling and Experimental Analysis of the Transient Overvoltages on Machine Windings Fed by PWM Inverters," 2017 12th International Conference on Power Systems Transients (IPST'17).

[10] M. K. Hussain and P. Gomez, "Equivalent representation of machine winding in frequency domain model for fast transient studies," 2017 IEEE Power and Energy Conference at Illinois (PECI), pp. 1-6.

[11] M. K. Hussain and P. Gomez, "Optimal filter tuning to minimize the transient overvoltages on machine windings fed by PWM inverters," 2017 IEEE North American Power Symposium (NAPS), 2017, pp. 1-6.

[12] A. Merouchi, E. David, F. Baudoin, D. Mary and I. Fofana, "Optimization of the electrical properties of epoxy-SiC composites for stress-grading application," 2015 IEEE Conference on Electrical Insulation and Dielectric Phenomena (CEIDP), pp. 713-716

[13] A. Naeini, E. A. Cherney and S. H. Jayaram, "Effect of conductivity on the thermal and electrical properties of the stress grading system of an inverter-fed rotating machine," IEEE Transactions on Dielectrics and Electrical Insulation, vol. 26, no. 1, pp. 179-186, Feb. 2019.

[14] G. C. Stone, E. A. Boulter, I. Culbert, H. Dhirani, Electrical Insulation for Rotating Machines Design, Evaluation, Aging, Testing, and Repair, Canada: John Wiley & Sons, Inc., 2004.

[15] M. K. Hussain and P. Gomez, "Modeling of machine coils under fast front excitation using a non-uniform multiconductor transmission line approach," 2016 IEEE North American Power Symposium (NAPS), pp. 1-6.

[16] P. Gomez, P. Moreno and J. L. Naredo, "Frequency-domain transient analysis of nonuniform lines with incident field excitation," IEEE Transactions on Power Delivery, vol. 20, no. 3, pp. 2273-2280, July 2005.

[17] P. Gómez and F. A. Uribe, "The numerical Laplace transform: An accurate technique for analyzing electromagnetic transients on power system devices," International Journal of Electrical Power & Energy Systems, vol. 31, no. 2–3, pp. 116–123, Feb. 2009.

[18] Introduction to COMSOL Multiphysics 5.5, COMSOL, 2019.

[19] Kai Zhou, Li Wan & Xutao Li (2013) Aging Characteristics of Inter-turn Insulation of Form-wound Stator Windings of Inverter-fed AC Motors, Electric Power Components and Systems, 41:13, 1280-1293

[20] D. Dung Le and D. -C. Lee, "Reduction of Half-Arm Current Stresses and Flying-Capacitor Voltage Ripples of Flying-Capacitor MMCs," in IEEE Access, vol. 8, pp. 180076-180086, 2020

[21] M. S. Moonesan, "A Study of Medium and High Voltage Form-Wound Coil Turn-to-Turn Insulation of Converter Fed Rotating Machines", PhD thesis, University of Waterloo, 2016

[22] M. Ghassemi, "Accelerated insulation aging due to fast, repetitive voltages: A review identifying challenges and future research needs," IEEE Trans. on Dielectrics and Electrical Insulation, vol. 26, no. 5, pp. 1558-1568, Oct. 2019